

Preprint Alberta-Thy-29-94. setgray (DRAFT)

The Deuteron Spin Structure Functions in the Bethe-Salpeter Approach and the Extraction of the Neutron Structure Function $g_1^n(x)$ ¹.

A.Yu. Umnikov, L.P. Kaptari[†], K.Yu. Kazakov[‡]
and F.C. Khanna

*Theoretical Physics Institute, Physics Department, University of Alberta,
Edmonton, Alberta T6G 2J1,
and TRIUMF, 4004 Wesbrook Mall, Vancouver, B.C. V6T 2A3, Canada*

[†]*Bogoliubov's Laboratory of Physics, JINR, Dubna, 141980 Russia*

[‡]*Far Eastern State University, Vladivostok, 690000 Russia*

Abstract

The nuclear effects in the spin-dependent structure functions g_1^D and b_2^D are calculated in the relativistic approach based on the Bethe-Salpeter equation with a realistic meson-exchange potential. The results of calculations are compared with the non-relativistic calculations. The problem of extraction of the neutron spin structure function, g_1^n , from the deuteron data is discussed.

1. PRELIMINARIES

In this talk we present a relativistic approach to the deep inelastic lepton scattering on the deuteron based on the Bethe-Salpeter (BS) equation within a realistic meson-exchange model. The method is developed in refs. [1, 2] and now we apply it to the deep inelastic scattering with polarized particles. We calculate the leading twist spin-dependent structure functions (SF) of the deuteron, g_1^D and b_2^D [3], and we discuss the extraction of the neutron SF g_1^n from deuteron data. This investigation is partially motivated by a number of existing and forthcoming experiments on the deep inelastic scattering of leptons by deuterons (SLAC, CERN, DESY, CEBAF). A covariant theory of this process will be useful in the analysis of the experimental data.

¹Talk given at the SPIN'94 International Symposium, September 15-22, 1994, Bloomington, Indiana.

2. THE BETHE-SALPETER AMPLITUDE FOR THE DEUTERON

An accurate description of both the NN -interaction at energies up to ~ 1 GeV, and the basic properties of the deuteron, can be provided within the meson-nucleon theory [4, 5]. The covariant description is based on the BS equation or its various approximations. We use the ladder approximation for the kernel of the BS equation [4]:

$$\Phi(p, P_D) = i\hat{S}(p_1) \cdot \hat{S}(p_2) \cdot \sum_B \int \frac{d^4 p'}{(2\pi)^4} \cdot \frac{g_B^2 \Gamma_B^{(1)} \otimes \Gamma_B^{(2)}}{(p - p')^2 - \mu_B^2} \cdot \Phi(p', P_D), \quad (1)$$

where μ_B is the mass of meson B ; Γ_B is the meson-nucleon vertex, corresponding to the meson B , $\hat{S}(p) = (\hat{p} - m)^{-1}$, m is the nucleon mass. This equation is solved, using the technique described in ref. [1].

The meson parameters, such as masses, coupling constants, cut-off parameters are taken similar to those in ref. [4], with a minor adjustment of the coupling constant of the scalar σ -meson so as to provide a numerical solution of the BS equation. All parameters are presented in Table 1, where coupling constants are shown in accordance with our definition of the meson-nucleon form-factors, $F_B(k) = (\Lambda^2 - \mu_B^2)/(\Lambda^2 - k^2)$.

The deuteron amplitude is normalized by using the conserved vector current:

$$J_\mu(0) = \langle P_D | \psi \gamma_\mu \psi | P_D \rangle = 2P_{D\mu}. \quad (2)$$

For the analysis of the processes with the polarized deuterons an important characteristic of the deuteron wave functions is the probability of the D -wave,

Table 1. Parameters of the model

meson B	coupling constants $g_B^2/(4\pi); [g_v/g_t]$	mass μ_B , GeV	cut-off Λ , GeV	isospin
σ	12.2	0.571	1.29	0
δ	1.6	0.961	1.29	1
π	14.5	0.139	1.29	1
η	4.5	0.549	1.29	0
ω	27.0; [0]	0.783	1.29	0
ρ	1.0; [6]	0.764	1.29	1
$m = 0.939$ GeV, $\epsilon_D = -2.225$ MeV				

\mathcal{P}_D , which varies in the range 3–6% for realistic potentials. Since the components of the BS amplitude do not have a direct probability interpretation, we consider the matrix element of the axial current on the deuteron state with the total momentum projection $M = 1$:

$$J_\mu^5(0) = \langle P_D | \bar{\psi} \gamma_5 \gamma_\mu \psi | P_D \rangle_{M=1} \quad (3)$$

$$J_3^5(0) \equiv \int_0^\infty n_{spin}^{BS}(|\mathbf{p}|) |\mathbf{p}|^2 d|\mathbf{p}|, \quad (4)$$

which corresponds in the non-relativistic limit to the mean value of the spin projection:

$$\begin{aligned}\langle P_D | \sigma_3 | P_D \rangle_{M=1} &= \int_0^\infty n_{spin}^{n.r.}(|\mathbf{p}|) |\mathbf{p}|^2 d|\mathbf{p}| = 1 - \frac{3}{2} \mathcal{P}_D, \\ n_{spin}^{n.r.}(|\mathbf{p}|) &= u^2(|\mathbf{p}|) - \frac{1}{2} w^2(|\mathbf{p}|).\end{aligned}\quad (5)$$

Our calculation of the matrix element (4) gives $J_3^5(0) = 0.922$, from which we get an approximate estimate of $\mathcal{P}_D^{BS} \approx 5.2\%$ in reasonable agreement with the estimate $\mathcal{P}_D^{BS} = 4.8\%$ from ref. [4] (compare, also, with $\mathcal{P}_D = 4.3\%$ and $\mathcal{P}_D = 5.9\%$ for Bonn and Paris potentials, respectively). Note, that accuracy of such a computations of the D -wave admixture from the (4) is of the order of the $\sim \langle p^2 \rangle / m^2$, i.e. $\sim 1\%$.

The matrix elements (2) and (3) contain the explicit integration over the relative 4-momentum. To compare our results with the non-relativistic case, we define the charge density $n_{ch.}^{BS}(|\mathbf{p}|)$ in the deuteron as a primitive function in (2) and (4) prior the integration on the modulus of the 3-momentum:

$$\langle P_D | \bar{\psi} \gamma_\mu \psi | P_D \rangle \equiv \int_0^\infty n_{ch.}^{BS}(|\mathbf{p}|) |\mathbf{p}|^2 d|\mathbf{p}|, \quad (6)$$

which corresponds to the non-relativistic charge density:

$$n_{ch.}^{n.r.}(|\mathbf{p}|) = u^2(|\mathbf{p}|) + w^2(|\mathbf{p}|), \quad (7)$$

where $u(|\mathbf{p}|)$ and $w(|\mathbf{p}|)$ are S - and D -waves components of the deuteron wave function. Similarly the spin density $n_{spin}^{BS}(|\mathbf{p}|)$ is defined from eq. (4). The charge and spin densities are compared with those obtained with wave functions of the Paris [7] and Bonn [6] potentials in Fig. 1 and 2, respectively. All calculations are in a reasonable agreement in the non-relativistic region, up to $|\mathbf{p}| \sim m$.

3. THE DEEP INELASTIC SCATTERING ON THE POLARIZED DEUTERON

To calculate the structure functions (SF) of the deuteron we use the OPE method within the effective meson-nucleon theory [10, 11, 1]. This method allows us to calculate SF in terms of the Wick rotated BS amplitude [1, 2]. Neglecting possible "off-mass-shell" corrections to the deuteron SF [8, 9], we obtain the deuteron SF in the convolution form. For two leading twist spin-dependent SF of the deuteron, g_1^D and b_2^D , [3] we have:

$$g_1^D(x) = \int_0^1 f_5^{N/D}(\xi) g_1^N(x/\xi) \frac{d\xi}{\xi}, \quad (8)$$

$$b_2^D(x) = \int_0^1 \Delta f^{N/D}(\xi) F_2^N(x/\xi) d\xi, \quad (9)$$

where g_1^N and F_2^N are isoscalar nucleon SF. The moments of the effective distribution functions, $f_5^{N/D}$ and $\Delta f^{N/D}$ are the matrix elements of the leading twist operators on the deuteron states:

$$\mu_n(f) = \int_0^1 x^{n-1} f(x) dx, \quad (10)$$

$$\mu_n(f_5^{N/D}) = \frac{1}{2M_D^n} \int \frac{d^4 p}{(2\pi)^4} p_{1+}^{n-1} \left[\bar{\Phi}_M(p) \gamma_+^{(1)} \gamma_5^{(1)} (p_2 \gamma^{(2)} - m) \Phi_M(p) \right] \Big|_{M=1}, \quad (11)$$

$$\begin{aligned} \mu_n(\Delta f^{N/D}) = \frac{1}{2M_D^n} \int \frac{d^4 p}{(2\pi)^4} p_{1+}^{n-1} \\ \left\{ \left[\bar{\Phi}_M(p) \gamma_+^{(1)} (p_2 \gamma^{(2)} - m) \Phi_M(p) \right] \Big|_{M=0} - \left[\dots \right] \Big|_{M=1} \right\}, \end{aligned} \quad (12)$$

where the kinematical variables in the rest frame are defined by

$$p = (p_0, \mathbf{p}), \quad P_D = (M_D, \mathbf{0}), \quad p_1 = \frac{P_D}{2} + p, \quad p_2 = \frac{P_D}{2} - p, \quad (13)$$

where M_D is the deuteron mass, $p_+ = p_0 + p_3$, $\gamma_+ = \gamma_0 + \gamma_3$ and we use deep inelastic kinematics: $pq \approx q_0(p_0 + p_3)$.

The explicit form of the effective distribution functions, $f_5^{N/D}$ and $\Delta f^{N/D}$ is defined by the inverse Mellin transform of (11) and (12). These distributions satisfy normalization conditions:

$$\int_0^1 f_5^{N/D}(\xi) d\xi = J_3^5(0), \quad \int_0^1 \Delta f^{N/D}(\xi) d\xi = 0. \quad (14)$$

Using the distribution functions, $f_5^{N/D}$ and $\Delta f^{N/D}$, and realistic parametrizations of the nucleon SF, g_1^N [12] and F_2^N [11], we calculate the deuteron SF g_1^D and b_2^D . The results of calculation are presented on Figs. 3 and 4. In Fig. 3 nuclear effects in g_1^D calculated within BS approach (solid curve) are compared with non-relativistic calculation [13, 14] with Bonn wave function. The non-relativistic calculation including the Fermi motion of polarized nucleons and binding effects (dashed curve) is in reasonable agreement with the relativistic calculations (solid curve). At the same time both these curves differ from non-relativistic impulse approximation (dotted), which does not include binding effects. The SF b_2^D calculated in relativistic and non-relativistic approaches is presented in Fig. 4. Similar to the case of the g_1^D , there is no special relativistic effect in b_2^D . The models are slightly distinguishable in view of different admixture of D -wave and minor variations of the nucleon momentum distributions.

4. ON THE EXTRACTION OF THE NEUTRON SF.

Mathematically the problem of extraction of the neutron SF from the deuteron data is formulated as a problem to solve the inhomogeneous integral equation (8) for the neutron SF with a model kernel $f_5^{N/D}$ and experimentally measured left hand side², g_1^D .

Recently we proposed a method to extract the neutron SF from the deuteron data within any model, giving deuteron SF in the form of a "convolution integral plus/minus additive corrections" [15]. The principal advantages of the method, compared with the smearing factor method, are the following. (i) Only analyticity of the SF need be assumed, (ii) the method allows us to elaborate on the spin-dependent SF, where the traditional smearing factor method does not work.

As an example, we apply our method to the SMC data [16]. The resulting nucleon functions are presented in fig. 5 (solid curves). It is clear that due to a singular behavior of the ratio g_1^D/g_1^N the nucleon SF g_1^N cannot be obtained by the smearing factor method. As a more practical result we can report that even in the experimentally restricted region of x the following integral relation is valid with high accuracy:

$$\int_{0.006}^{0.6} g_2^D(x) dx \cong (1 - \frac{3}{2}\mathcal{P}_D) \cdot \int_{0.006}^{0.6} g_2^N(x) dx, \quad (15)$$

5. CONCLUSIONS

We have presented a description of the spin-dependent deep inelastic lepton-deuteron scattering based on the Bethe-Salpeter formalism within an effective meson-nucleon theory. In particular,

1. The spinor-spinor Bethe-Salpeter equation for the deuteron is solved in the ladder approximation for a realistic meson exchange potential.
2. The leading twist spin-dependent structure functions, g_1^D and b_2^D , of the deuteron are calculated in terms of the Bethe-Salpeter amplitude.
3. Numerical results of the calculations of the deuteron structure functions g_1^D and b_2^D in the Bethe-Salpeter formalism are presented. It is found that results are in qualitative agreement with previous non-relativistic calculation.
4. A method to extract the neutron structure function, g_1^N , from the deuteron and proton data is suggested.

The reasonable quantitative agreement of the presented calculations of the deuteron SF at $x < 1$ in the non-relativistic and relativistic approaches confirms the expectation that

²Depending of the model, some additive corrections could be taken into account [15].

these approaches have to give similar results within the boundaries of validity of the non-relativistic approximation. However, it does not imply that the relativistic effects in the deuteron SF are negligible in general. It only shows that in a slightly relativistic system such as the deuteron we should find *special* kinematic conditions of the experiment to display the relativistic effects. We could expect non-trivial relativistic phenomena at $x > 1$, where the precise evaluation of the SF is important for QCD analysis of the experimental data. The behavior of the nuclear SF $\sim (1 - x_N)^\gamma$ as $x_N \rightarrow 1$ may lead to errors.

References

- [1] A.Yu. Umnikov and F.C. Khanna, Phys. Rev. **C49** (1994) 2311.
- [2] A.Yu. Umnikov, L.P. Kaptari, K.Yu. Kazakov and F.C. Khanna, Phys. Lett. **B334** (1994) 163.
- [3] P. Hoodbhoy, R.L. Jaffe and A. Manohar, Nucl. Phys. **B312** (1989) 571; R.L. Jaffe and A. Manohar, Nucl. Phys. **B321** (1989) 343.
- [4] M.J. Zuilhof and J.A. Tjon, Phys. Rev. **C22** (1980) 2369.
- [5] F. Gross, J.W. Van Orden and K. Holinde, Phys. Rev. **C45** (1992) 2094.
- [6] R. Machleidt, K. Holinde and Ch. Elster, Phys. Rep. **149** (1987) 1.
- [7] M. Lacombe et al, Phys. Rev. **C21** (1980) 861.
- [8] W. Melnitchouk, A.W. Schreiber and A.W. Thomas, Phys. Rev. **D49** (1994) 1183.
- [9] S.A. Kulagin, G. Piller and W. Weise, Preprint TPR-94-02, Regensburg; Preprint ADP-94-1/T144, Adelaide, 1994.
- [10] B.L. Birbrair, E.M. Levin and A.G. Shuvaev, Nucl. Phys. **A496** (1989) 704.
- [11] L.P. Kaptari, K.Yu. Kazakov and A.Yu. Umnikov, Phys. Lett. **B293** (1992) 219; L.P. Kaptari, A.Yu. Umnikov and B. Kämpfer, Phys. Rev. **D47** (1993) 3804.
- [12] A. Schäfer, Phys. Lett. **B208** (1988) 175.
- [13] L.P. Kaptari, K.Yu. Kazakov, A.Yu. Umnikov and B. Kämpfer, Phys. Lett. **B321** (1994) 271; **B322** (1994) E473.
- [14] L.P. Kaptari, A.Yu. Umnikov, C. Ciofi degli Atti, S. Scopetta and K.Yu. Kazakov, Preprint DFUPG 92/94, Perugia, 1994.
- [15] A.Yu. Umnikov, F.C. Khanna and L.P. Kaptari, Z. Phys. **A348** (1994) 211.
- [16] SM Collab., B. Adeva et al., Phys. Lett **B302** (1993) 534.

Figure captions:

Figure 1. The charge density calculated in different models (see text).

Figure 2. The spin density calculated in different models (see text).

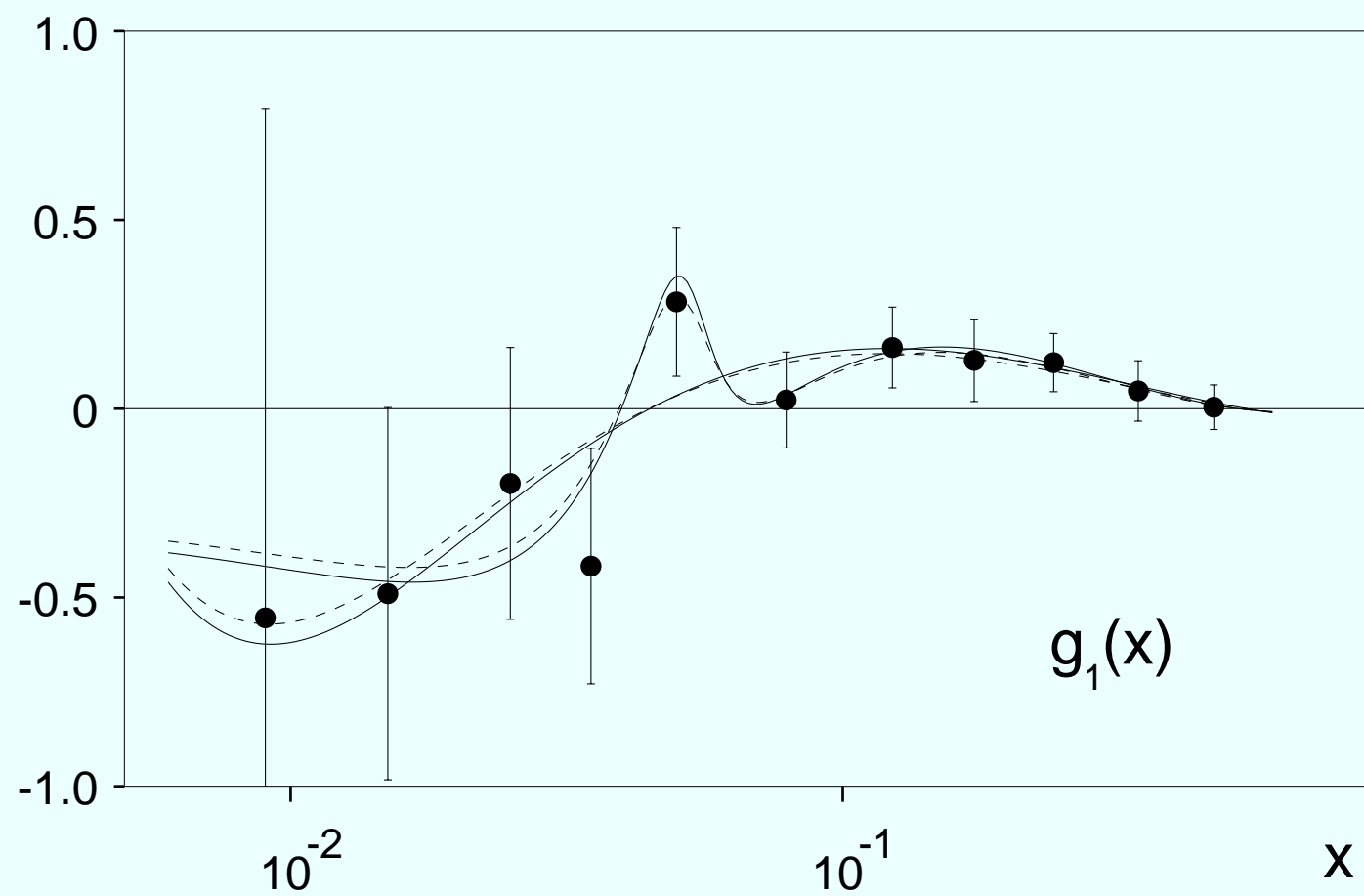
Figure 3. The ratio of the deuteron and nucleon SF, g_1^D/g_1^N .

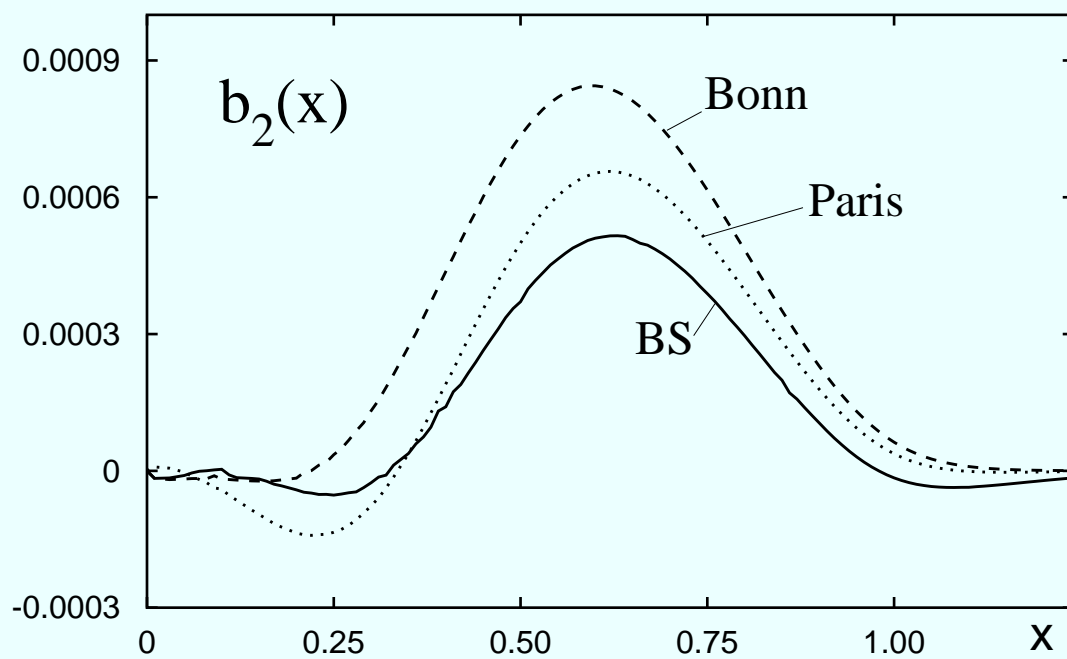
Figure 4. The deuteron SF b_2 calculated in different models (see text)

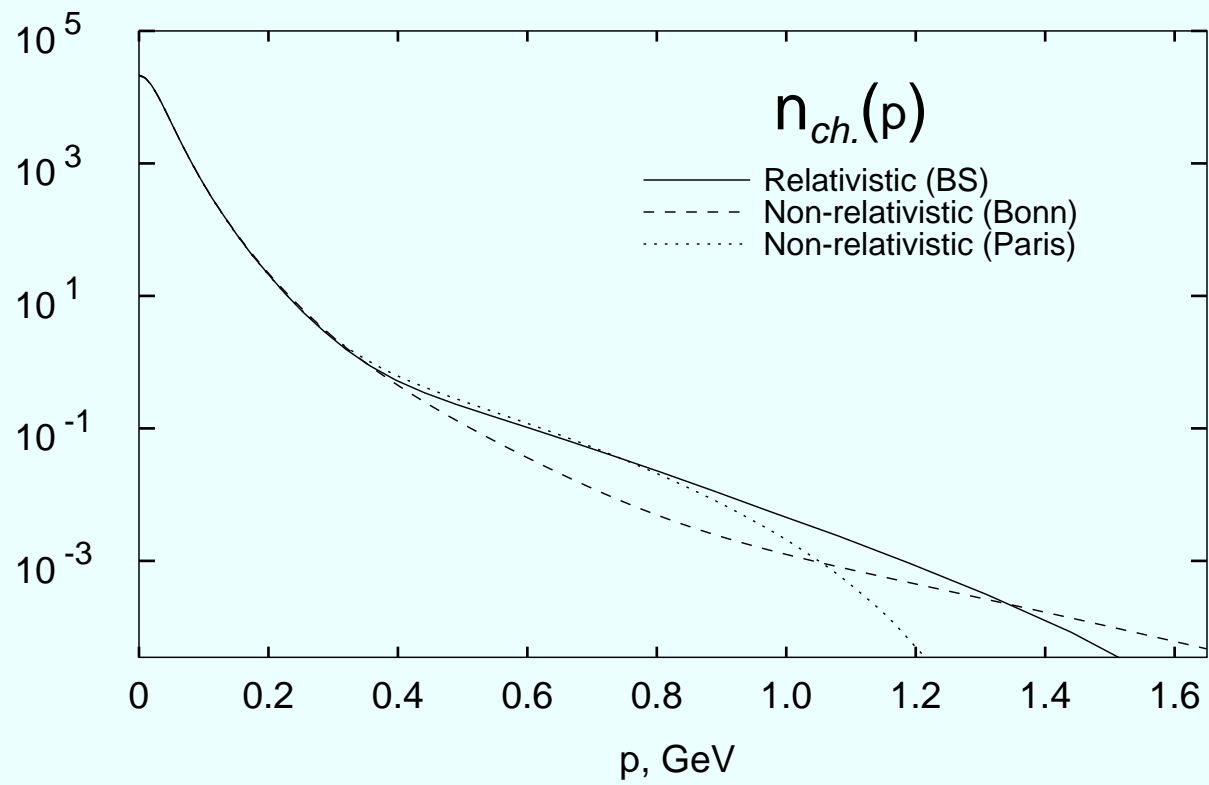
Figure 5. The SF g_1 of deuteron (dashed lines) and nucleon (solid lines) for two different parametrizations of data.

This figure "fig1-1.png" is available in "png" format from:

<http://arXiv.org/ps/hep-ph/9410241v1>







This figure "fig1-2.png" is available in "png" format from:

<http://arXiv.org/ps/hep-ph/9410241v1>

This figure "fig1-3.png" is available in "png" format from:

<http://arXiv.org/ps/hep-ph/9410241v1>

This figure "fig1-4.png" is available in "png" format from:

<http://arXiv.org/ps/hep-ph/9410241v1>

This figure "fig1-5.png" is available in "png" format from:

<http://arXiv.org/ps/hep-ph/9410241v1>

